

Weak dimers and soft phonons on the β -SiC(100) surface

This article has been downloaded from IOPscience. Please scroll down to see the full text article.

2009 J. Phys.: Condens. Matter 21 182003

(<http://iopscience.iop.org/0953-8984/21/18/182003>)

View [the table of contents for this issue](#), or go to the [journal homepage](#) for more

Download details:

IP Address: 129.252.86.83

The article was downloaded on 29/05/2010 at 19:29

Please note that [terms and conditions apply](#).

FAST TRACK COMMUNICATION

Weak dimers and soft phonons on the β -SiC(100) surface

Daniel G Trabada¹ and José Ortega^{1,2}¹ Departamento de Física Teórica de la Materia Condensada, Universidad Autónoma, E-28049 Madrid, Spain² Department of Physics, West Virginia University, Morgantown, WV 26506, USAE-mail: jose.ortega@uam.es

Received 3 March 2009

Published 31 March 2009

Online at stacks.iop.org/JPhysCM/21/182003**Abstract**

We study the β -SiC(100) $c(4 \times 2) \leftrightarrow (2 \times 1)$ reversible phase transition, using first-principles molecular dynamics simulations to search for the ground state atomic structure as well as to investigate the dynamics of this surface. We find that this surface consists of weakly bonded asymmetric Si dimers that exhibit a complex atomic motion, associated with a surface soft phonon. This soft phonon is strongly coupled to the electrons in dangling bond states close to the Fermi level, explaining the observed insulator–metal transition. We identify the dynamical processes responsible for the phase transition and predict that this surface should undergo another reversible phase transition at low T .

The surfaces and interfaces of semiconductors have been extensively studied during the last 60 years with a great variety of experimental, theoretical and computational tools. As a result of this effort, many of their physical properties are well understood, and also some interesting new phenomena have been discovered. This is the case of the temperature-induced reversible phase transitions (RPTs) that have been observed in some of these systems (see, e.g., [1–10]). In these RPTs the translational symmetry of the surface changes reversibly as a function of T . This structural transition is often accompanied by an electronic insulator–metal (IM) transition.

The atomic mechanisms responsible for these RPTs have been under intense debate. Peierls instabilities and charge density wave formation [2–5, 11], order–disorder processes [7–9], soft phonons [10, 12–15], electron correlations [2, 3], dynamical fluctuations [15–17], etc, have all been proposed, these mechanisms not being mutually exclusive. From a fundamental point of view, two questions must be solved in order to understand these RPTs at a microscopic level: (1) what is the origin and precise atomic structure of the low T phase? and (2) which are the atomic dynamical processes that give rise to the structural (and eventually IM) transitions? The first question has already proven a difficult theoretical/computational

problem [2, 3, 14–16, 18–20] due to (i) the delicate energy differences between candidate atomic structures, (ii) the inaccuracies present in all first-principles methods and (iii) the complex energy landscape that has to be explored in order to find the relevant atomic geometries, which usually involve not obvious distortions from ideal structures. Once the first question is solved, first-principles molecular dynamics (MD) simulations may be performed in an attempt to answer the second.

In this paper we analyse the puzzling β -SiC(100) $c(4 \times 2)$ case. This surface undergoes a reversible phase transition to a (2×1) symmetry when the temperature is increased above $T_c \sim 670$ K which is accompanied by an IM electronic transition [6]. Although this surface has been intensively studied [6, 21–32], the $c(4 \times 2)$ atomic geometry, the nature of the 2×1 high temperature phase and the origin of the IM transition are not well understood. Two main structural models have been discussed regarding the β -SiC(100) $c(4 \times 2)$ atomic structure, with two different Si coverages (θ) above the last C layer. In the AUDD model [22], the surface is terminated by an Si monolayer ($\theta = 1$), the Si atoms forming alternately up and down symmetric dimers, while the MRAD model [31] consists of asymmetric Si dimers on top of an Si-terminated surface ($\theta = 1.5$). While the experimental evidence [21–29]

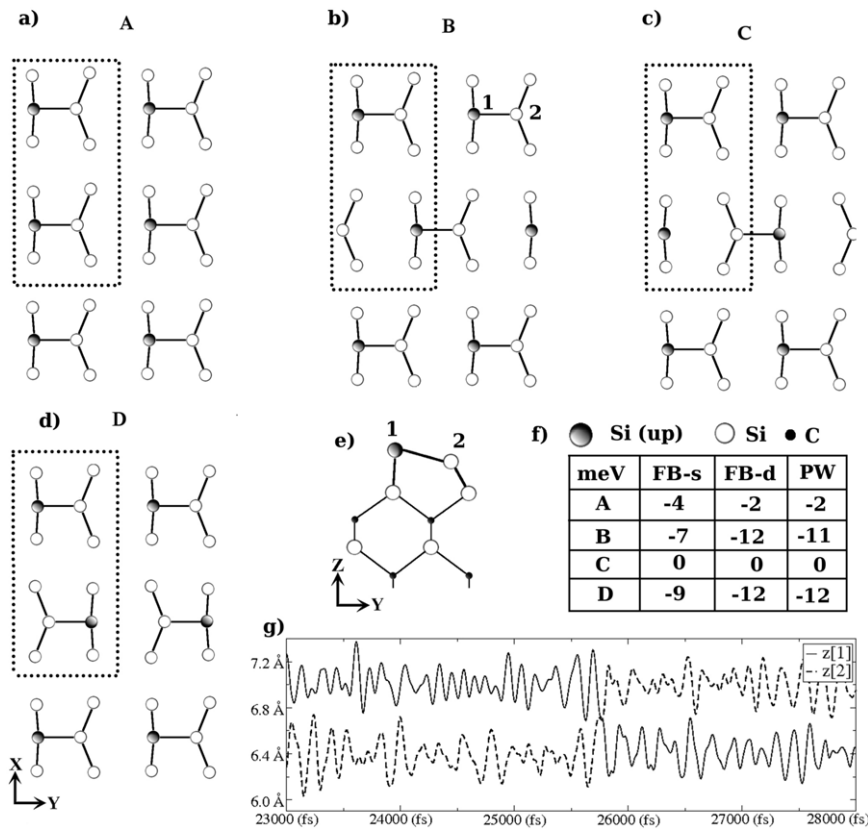


Figure 1. ((a)–(d)) Top view of the $\theta = 1.5$ structural models A–D, showing the Si atoms of the top two layers. The 4×2 unit cell is outlined. The grey circle indicates the top atom of the Si dimer. (e) Side view. (f) Table with the relative energies for structures A–D, in meV per 1×1 unit cell as calculated with the different codes. (g) Fragment of the time evolution of the vertical coordinate z for atoms 1 and 2 (see (b) and (e)) in an MD run at $T \sim 1000$ K, showing the flipping of a dimer.

favours the AUDD over the MRAD, density functional theory (DFT) calculations indicate that the AUDD structure is not stable without artificially introducing a significant strain in the calculations [29–32]. In this work we study the ground state geometry as well as the atomic dynamics of this surface using DFT MD techniques [35, 36], complemented by DFT plane-wave (PW) calculations [37]. We find new low energy structures for both $\theta = 1.0$ and 1.5 . Our MD simulations show that the $\theta = 1.5$ structures present an atomic motion with very stable Si dimers that cannot explain the observed reversible transition to a 2×1 symmetry. In the case of $\theta = 1.0$ the Si-dimer bonds are weak and display a complex dynamical behaviour associated with a surface soft phonon. We show that this soft phonon is strongly coupled to the electrons in frontier orbitals (dangling bonds), explaining the observed IM transition. In our MD simulations we identify the dynamical processes responsible for the $c(4 \times 2) \leftrightarrow (2 \times 1)$ transition. Our calculations also predict that this surface should present another transition to lower structural symmetry at low T .

The FIREBALL (FB) code [35, 36] has proven very useful in our previous studies for the $\text{Sn/Ge}(111)\text{-}\sqrt{3} \times \sqrt{3} \leftrightarrow 3 \times 3$ [12, 16, 20] and $\text{In/Si}(111)\text{-}4 \times 1 \leftrightarrow 8 \times 2$ [14, 15] phase transitions. Due to the computational efficiency of this technique, first-principles MD simulations can be easily performed to search for new energy minima [14, 20] and to explore the atomic dynamics [12, 15, 16]. The PW method

is much more demanding in computational resources, and in this work it has been used to refine the FB findings. In the present case, we have used two different basis sets of numerical atomic-like orbitals for the FB calculations: an optimized simple (sp^3) basis (FB-s) or a double ($sp^3s^*p^3$) basis (FB-d). In order to optimize the simple basis set we performed calculations for bulk SiC, Si and C and selected the basis set that yielded lowest total energies and best equilibrium lattice parameters [38]. For the PW calculations we use ultrasoft pseudopotentials and a PW cutoff energy of 280 eV. In both codes we have used the LDA exchange–correlation functional [39]. In our calculations the β -SiC(100) is modelled by means of 8 SiC layers and H atoms saturating the lowest C layer; the lowest two SiC layers are fixed at bulk positions. We have used a 4×2 surface unit cell and 8 special k -points to sample the surface Brillouin zone. We have considered two different Si coverages, $\theta = 1.5$ and 1.0 . In all these calculations we use the corresponding equilibrium lattice parameter³ $a = 4.40$ Å (FB-s and FB-d) or $a = 4.32$ Å (PW), i.e. no strain is imposed on the surface. The atomic dynamics are explored by performing long ($\sim 500\,000$ fs) FB MD simulations for different temperatures.

Figure 1 shows the different structures we have analysed for $\theta = 1.5$: figure 1(b) corresponds to the MRAD

³ The SiC experimental lattice parameter is $a = 4.36$ Å.

model [31], while the others are variants of it corresponding to a different arrangement of the asymmetric Si dimers. All these structures present very similar total energies (see the table in figure 1); interestingly the lowest energy structure is not the original MRAD model but figure 1(d), which presents a 4×2 symmetry. The dimer bond distance d is similar in all these structures, $d \sim 2.3 \text{ \AA}$, which corresponds to the formation of a strong dimer bond. Notice the excellent agreement for the energy differences between the different codes.

In our first-principles MD simulations for these structures we find that the top Si dimers are very stable. At $T \sim 1000 \text{ K}$ (see figure 1(g)) the Si dimers occasionally flip, changing between their two possible tilted positions, without breaking the strong dimer bond, while no dimer flip is observed in our simulations for $T \sim 700 \text{ K}$ (not shown). Due to this flip-flop motion at height T the surface would fluctuate locally between structures B and C, or between structures D and A, presenting on average a $c(4 \times 2)$ or 2×2 , symmetry, but not the 2×1 symmetry observed at high T . A possible explanation of the 2×1 phase with these models would require the breaking of the strong Si dimers, a process that in view of our results is not very likely.

We turn our attention now to the $\theta = 1.0$ case. Let us consider first the β -SiC(100)- 1×1 surface. In this ideal surface the distance between Si atoms is 3.1 \AA , and each Si atom of the top layer presents two dangling bonds. In spite of this, the surface is semiconducting with a small energy gap. Due to this remarkable property, strong Si-dimer bonds are not required to stabilize this surface. In fact, the lowest energy structure found so far for $\theta = 1.0$ is a 2×1 reconstruction with weak Si dimers, $d \sim 2.7 \text{ \AA}$; this 2×1 surface is only a few meV lower in energy than the 1×1 [31–34].

Figure 2 shows the most stable structures we have found in our MD search for $\theta = 1.0$; in the PW and FB-s calculations the most stable is the 4×1 structure shown in figure 2(a). In this structure Si atoms of the top layer form chains of four atoms along the x direction (atoms 1–4 in figure 2(a)); within this chain, Si atoms 1–2 and 3–4 form weakly bonded dimers that are slightly asymmetric, $\Delta z \sim 0.08 \text{ \AA}$. The dimer bond length is $d = 2.61 \text{ \AA}$ (PW) or 2.70 \AA (FB-s); the distance between atoms 2 and 3 is $\sim 2.9 \text{ \AA}$, which is shorter than the distance between Si atoms in the ideal 1×1 surface, showing that there is some bonding interaction between dimers 1–2 and 3–4 (dotted lines in figure 2). This 4×1 structure is significantly lower in energy than the 1×1 surface, by 60 meV (PW) or 85 meV (FB-s), per 1×1 unit cell. Interestingly, in our FB-d calculations the minimum energy structure presents instead a 4×2 symmetry; this 4×2 structure can be obtained from the previous 4×1 by tilting the four-Si-atom chains in alternate orientations along the y direction, as shown in figures 2(b) and (c). This 4×2 distortion yields up and down dimers, in similarity to the AUDD model, with the difference that the dimers are asymmetric. The up-dimer is, on average, $\sim 0.2 \text{ \AA}$ above the down-dimer with dimer bond distances $d = 2.8$ (up) and 2.6 \AA (down).

These two minimum energy structures are clearly related. In figure 3 we analyse the energy along a path joining them.

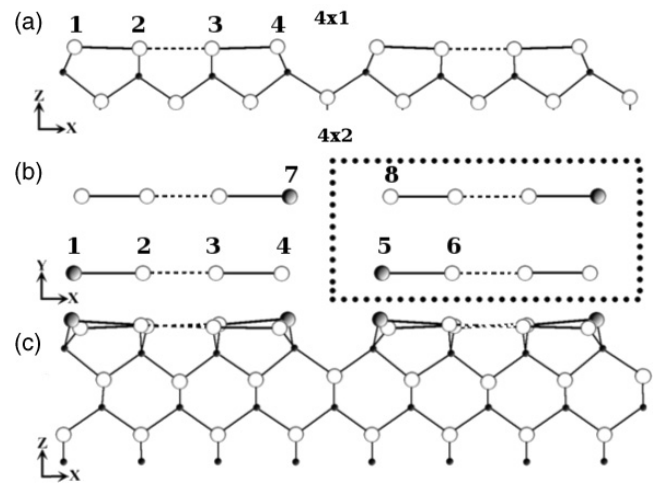


Figure 2. Lowest total energy models for $\theta = 1.0$. (a) and (c) are side views for the 4×1 and 4×2 structures. (b) Top view of the 4×2 structure. The grey circles indicate the highest Si atoms. The 4×2 unit cell is shown.

As shown in figure 3, these 4×1 and 4×2 structures are connected through a *soft phonon distortion*, both structures presenting very similar total energies and practically no energy barrier between them, as calculated by the three calculational methods. Figure 3 also shows the strong coupling between this distortion and the electrons in dangling bond orbitals close to the Fermi level. As we move along the distortion (i.e. along the x axis in figure 3), an electronic energy gap E_g opens at the Fermi level. At the 4×2 minimum ($x = 0.22 \text{ \AA}$) this gap is $E_g = 0.33 \text{ eV}$, this value increasing as we move further along this curve, e.g. $E_g = 0.82 \text{ eV}$ for $x = 0.38 \text{ \AA}$, see figure 3. We also mention that, due to this soft phonon, the 4×1 structure is unstable even in our FB-s simulations, in which the system evolves jumping between different 4×2 structures⁴.

Our MD simulations at different T for $\theta = 1.0$ show that the top Si atoms display a complex dynamical behaviour, their vertical coordinates z and dimer bond lengths d presenting large variations as a function of time. For example, in figure 4(b) the bond length d for dimers 1–2 and 3–4 oscillates between ~ 2.4 and 3.3 \AA [32]. In these MD simulations we have found two different processes that allow the system to jump between equivalent ground state 4×2 structures: (a) *up-down dimer* fluctuations, in which dimers interchange heights, up dimers becoming down dimers and vice versa, see figure 4(a); (b) *trench* fluctuations, in which the position of the trench (e.g. between atoms 4–5 and 7–8 in figure 2) changes its place; an example is shown in figure 4(b), where dimer 3–4 breaks its weak bond with dimer 1–2 (dotted line in figure 2) and moves to the right closer to dimer 5–6 in such a way that the trench is now placed between atoms 2–3.

These results suggest the following explanation for the β -SiC(100) $c(4 \times 2) \leftrightarrow (2 \times 1)$ transition. At very low T Si atoms form weakly bonded up and down asymmetric dimers.

⁴ There are eight degenerate 4×2 structures, depending on the position of the trench and on the tilting orientation of the Si dimers.

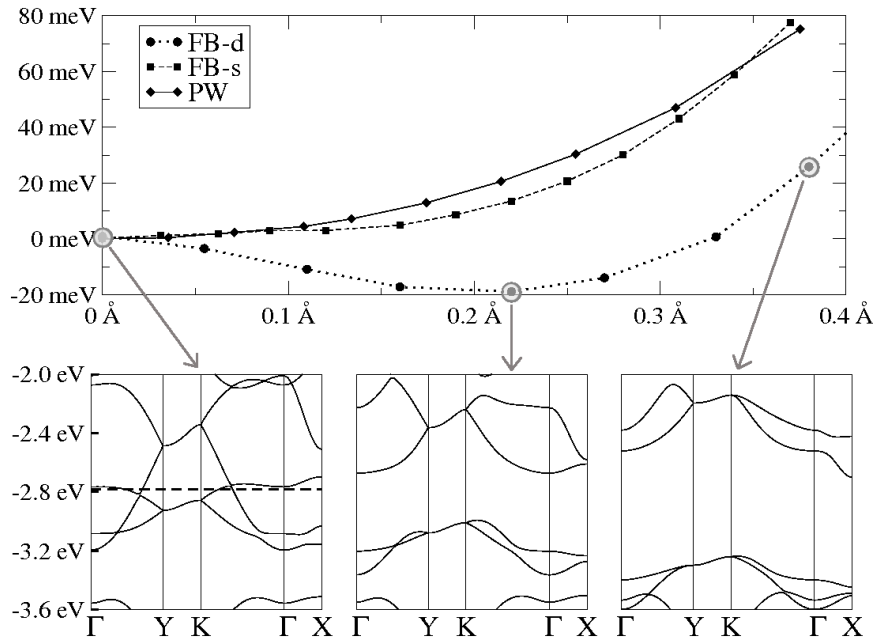


Figure 3. (Up) Energy (in meV/ $l \times 1$) of the distortion from the 4×1 to the 4×2 structure, see figure 2. In these calculations atoms 4, 5, 7 and 8 (figure 2(b)) are fixed at different positions along a path between the 4×1 to the 4×2 structure, and the rest of the atoms in the unit cell are relaxed. The x axis represents the average of the displacements from the 4×1 of atoms 4, 5, 7 and 8. (Down) Surface band structures showing the opening of a gap at the Fermi level (dashed line) along this distortion; the arrows connect the points in the energy curve with the corresponding band structures.

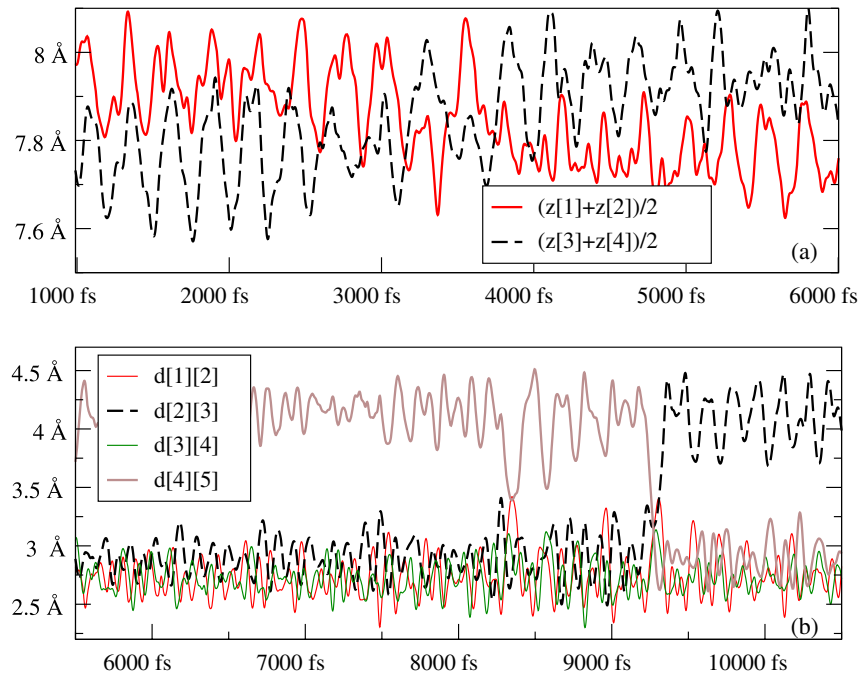


Figure 4. Fragments of MD simulations showing the fluctuations discussed in the text. (a) Time evolution of the average vertical coordinate for dimers 1–2 and 3–4 (figure 2), for $T \sim 600$ K, showing an up/down dimer fluctuation. (b) Time evolution of the distance between atoms 1–2, 2–3, 3–4 and 4–5 (figure 2) for $T \sim 550$ K: the trench, initially between atoms 4 and 5, changes to be between atoms 2–3. (This figure is in colour only in the electronic version)

As the temperature is increased, the $c(4 \times 2)$ phase appears as a result of the motion of these atoms, which move with large displacements both in their vertical coordinates and dimer bond lengths. This motion gives rise, on average, to the observed

$c(4 \times 2)$ phase (i.e. a *dynamical AUDD* model [22])⁵. A further increase in temperature promotes trench and up/down

⁵ Also, trench fluctuations might be activated before up/down fluctuations.

dimer fluctuations and thus a transition to an average 2×1 symmetry [6]. Due to the strong coupling of the electrons in the dangling bonds close to the Fermi level with two-dimensional lattice vibrations (see figure 3), at high T the system frequently visits metallic structures while jumping between different 4×2 structures, explaining the observed IM transition, in similarity to the In/Si(111)- $4 \times 1 \leftrightarrow 8 \times 2$ case [15, 40].

A comparison with other cases, such as Sn/Ge(111)- $\sqrt{3} \times \sqrt{3} \leftrightarrow 3 \times 3$ and In/Si(111)- $4 \times 1 \leftrightarrow 8 \times 2$, shows that these RPTs present similar features [12, 15], suggesting the following model for a reversible phase transition on clean and metal-adsorbed semiconductor surfaces.

- (i) Several equivalent ground state structures are originated from a high symmetry *ideal* structure by means of soft distortions; these distortions are strongly coupled to the electrons in frontier orbitals.
- (ii) At low T the system is frozen in one of these lower symmetry ground states.
- (iii) At high T , dynamical fluctuations between these structures give rise, on average (i.e. on the timescale of STM or LEED), to the observed high symmetry.
- (iv) Due to the underlying soft phonons, eventually the system frequently visits atomic configurations that are metallic while jumping between degenerate ground states [15, 40], resulting in the observed IM transitions.

In summary, we have investigated the β -SiC(100) $c(4 \times 2) \leftrightarrow (2 \times 1)$ surface using first-principles MD techniques. Our results indicate that the last layer of this surface consists of weakly bonded Si dimers that display a complex atomic motion. In this motion, two-dimensional lattice vibrations are strongly coupled to the electrons in frontier orbitals, explaining the insulator–metal transition observed at high T . We have found new minimum energy structures with (4×1) and (4×2) translational symmetry that are significantly lower in energy than the lowest energy structures found previously. We have also identified the atomic dynamical processes that produce the 2×1 phase at high T . Finally, we have proposed a model that may be of application to explain other reversible phase transitions on semiconductor surfaces.

We thank Professors F Flores, P Soukiassian and E G Michel for stimulating discussions. This work was funded by the Spanish MEC under contract no. MAT2007-06966.

References

- [1] Mascaraque A and Michel E G 2002 *J. Phys.: Condens. Matter* **14** 6005
- [2] Carpinelli J M, Weitering H H, Plummer E W and Stumpf R 1996 *Nature* **381** 398
- [3] Carpinelli J M *et al* 1997 *Phys. Rev. Lett.* **79** 2859
- [4] Yeom H W *et al* 1999 *Phys. Rev. Lett.* **82** 4898
- [5] Ahn J R, Yeom H W, Yoon H S and Lyo I W 2003 *Phys. Rev. Lett.* **91** 196403
- [6] Aristov V Y, Douillard L, Fauchoux O and Soukiassian P 1997 *Phys. Rev. Lett.* **79** 3700
- [7] Kevan S D and Stoffel N G 1984 *Phys. Rev. Lett.* **53** 702
- [8] Tabata T, Aruga T and Murata Y 1987 *Surf. Sci.* **179** L63
- [9] Kim Y K *et al* 2005 *Surf. Sci.* **596** L325
- [10] Brihuega I, Custance O, Pérez R and Gómez-Rodríguez J M 2005 *Phys. Rev. Lett.* **94** 046101
- [11] Aruga T 2006 *Surf. Sci. Rep.* **61** 283
- [12] Fariás D *et al* 2003 *Phys. Rev. Lett.* **91** 016103
- [13] Pérez R, Ortega J and Flores F 2001 *Phys. Rev. Lett.* **86** 4891
- [14] González C, Ortega J and Flores F 2005 *New J. Phys.* **7** 100
- [15] González C, Flores F and Ortega J 2006 *Phys. Rev. Lett.* **96** 136101
- [16] Ávila J *et al* 1999 *Phys. Rev. Lett.* **82** 442
- [17] Ortega J, Pérez R and Flores F 2002 *J. Phys.: Condens. Matter* **14** 5979
- [18] Riikonen S and Sánchez-Portal D 2007 *Phys. Rev. B* **76** 035410
- [19] Stekolnikov A A *et al* 2007 *Phys. Rev. Lett.* **98** 026105
- [20] Ortega J, Pérez R and Flores F 2000 *J. Phys.: Condens. Matter* **12** L21
- [21] Shek M L 1996 *Surf. Sci.* **349** 317
- [22] Soukiassian P *et al* 1997 *Phys. Rev. Lett.* **78** 907
- [23] Hara S *et al* 1990 *Surf. Sci.* **231** L196
- [24] Duda L *et al* 2000 *Phys. Rev. B* **61** R2460
- [25] Aristov V Y *et al* 1999 *Phys. Rev. B* **60** 16553
- [26] Benesch C, Merz H and Zacharias H 2001 *Surf. Sci.* **492** 225
- [27] Enriquez H *et al* 2000 *Appl. Surf. Sci.* **162–63** 559
- [28] Aristov V Y *et al* 2004 *Phys. Rev. B* **69** 245326
- [29] Tejada A *et al* 2007 *Phys. Rev. B* **75** 195315
- [30] Krüger P and Pollmann J 2006 *Phys. Rev. B* **73** 035327
- [31] Lu W, Krüger P and Pollmann J P 1998 *Phys. Rev. Lett.* **81** 2292
- [32] Catellani A *et al* 1998 *Phys. Rev. B* **57** 12255
- [33] Sabisch M *et al* 1996 *Phys. Rev. B* **53** 13121
- [34] Käckell P *et al* 1997 *Surf. Sci.* **391** L1183
- [35] Lewis J P *et al* 2001 *Phys. Rev. B* **64** 195103
- [36] Jelínek P *et al* 2005 *Phys. Rev. B* **71** 235101
- [37] Segall M D *et al* 2002 *J. Phys.: Condens. Matter* **14** 2717
- [38] Basanta M A *et al* 2007 *Comput. Mater. Sci.* **39** 759
- [39] Kohn W and Sham L J 1965 *Phys. Rev.* **140** A1133
- [40] González C, Guo J D, Ortega J, Flores F and Weitering H H 2009 *Phys. Rev. Lett.* **102** 115501